

The Role of Quantitative DCE-MRI and Diffusion-Weighted Imaging in Differentiating the Grade of Soft Tissue Sarcomas

Ahmet Peker¹ , Aytek Hüseyin Çeliksöz² , Hande Özen Atalay¹ , Enes Muhammed Cantürk¹ , Yunus Emre Şentürk¹ 

¹Department of Radiology, Koç University Hospital, İstanbul, Türkiye

²Department of Orthopedics and Traumatology, Koç University Hospital, İstanbul, Türkiye

Cite this article as: Peker A, Çeliksöz AH, Özen Atalay H, Canturk EM, Şentürk YE. The role of quantitative DCE-MRI and diffusion-weighted imaging in differentiating the grade of soft tissue sarcomas. *Cerrahpaşa Med J.* 2026, 50, 0074, doi: 10.5152/cjm.2026.25074.

What is already known on this topic?

- Diffusion-weighted imaging (DWI) and apparent diffusion coefficient (ADC) values are associated with soft tissue sarcoma (STS) grade, with lower ADC values linked to higher tumor aggressiveness.
- Dynamic contrast-enhanced magnetic resonance imaging (DCE-MRI) has been studied for characterizing soft tissue tumors, but its specific role in grading STS remains underexplored.
- Histological grading is essential for prognosis and treatment planning in STS, but current reliance on biopsy has known limitations such as sampling error and tumor heterogeneity.

What does this study add on this topic?

- This is the first study to comprehensively evaluate the combined role of quantitative DCE-MRI parameters and ADC values for grading STS.
- K_{trans_max} , AUC_{max} , and K_{trans_mean} values from DCE-MRI were significantly higher in high-grade STS, while ADC_{min} and ADC_{mean} values were significantly lower.
- The study shows that integrating DCE-MRI with DWI may provide a non-invasive and effective imaging-based approach for preoperative STS grading, potentially complementing or reducing the need for biopsy.

Abstract

Objective: Tumor grade is critical for prognosis, metastatic risk, and treatment planning in soft tissue sarcomas (STSs). This study evaluated the role of quantitative dynamic contrast-enhanced magnetic resonance imaging (DCE-MRI) parameters and diffusion-weighted imaging (DWI) in predicting STS grade.

Methods: Between March 2022 and February 2023, patients with histopathologically confirmed STS who underwent DCE-MRI and DWI were retrospectively included; those with prior therapy or liposarcoma were excluded. Two musculoskeletal radiologists (3 and 4 years of experience) reviewed the exams. Age, gender, and tumor diameter (LD) were recorded. Dynamic contrast-enhanced magnetic resonance imaging measurements were obtained from Ktrans maps, avoiding hemorrhagic, necrotic, and cystic areas. Regions of interest were placed over the most perfused region (max) and a broader area (mean). Parameters (K_{trans} , area under the curve [AUC], K_{ep} , V_e) and enhancement curves were documented. Apparent diffusion coefficient (ADC_{min} and ADC_{mean}) were measured from ADC maps. Soft tissue sarcomas were grouped by pathological grade (1-3) and as low (1-2) vs. high (3).

Results: Fourteen patients (3 females, 11 males) were included: 4 grade 1, 2 grade 2, and 8 grade 3. Mean age was 58.07 ± 16.35 years; mean LD 113.36 ± 36.87 mm. Inter-observer agreement was excellent for perfusion max values and ADC_{min} , and good for perfusion mean and ADC_{mean} . No significant differences were found in age or LD. Apparent diffusion coefficient (ADC_{mean}) ($P = .026$), ADC_{min} ($P = .029$), and AUC_{max} ($P = .047$) differed among grades. In low- vs. high-grade comparison, ADC_{mean} , ADC_{min} , K_{trans_max} , AUC_{max} , and K_{trans_mean} were significant.

Conclusion: Apparent diffusion coefficient (ADC_{min}), ADC_{mean} , AUC_{max} , K_{trans_max} , and K_{trans_mean} may support STS grading.

Keywords: Diffusion-weighted imaging, grading of sarcoma, perfusion MRI, soft tissue sarcoma

Introduction

Soft tissue sarcomas (STSs) are a rare group of malignancies associated with high recurrence and mortality rates.¹ Magnetic resonance imaging (MRI) plays a central role in the assessment of STS, serving as the most effective modality for defining tumor extent and aiding in preoperative planning and prognostication.²⁻⁵ Among the key prognostic factors, the histological type and grade of STS are particularly important in predicting metastatic potential and overall survival.^{6,7} Although biopsy remains the standard method for determining tumor grade, it has limitations—including inadequate sampling, tumor heterogeneity, and the risk of tumor cell seeding—which highlight the need for a more reliable, non-invasive approach to preoperative grading.⁶

Diffusion-weighted imaging (DWI) is commonly used for evaluating soft tissue lesions. It reflects the degree of water molecule diffusion, quantified by the apparent diffusion coefficient (ADC). Lower ADC values are generally associated with increased cellularity, a hallmark of malignant tissue, while higher ADC values typically indicate benign or less aggressive lesions due to freer water diffusion.⁷⁻¹⁰

Received: September 18, 2025 **Revision requested:** October 12, 2025 **Last revision received:** October 30, 2025

Accepted: November 27, 2025 **Publication date:** February 23, 2026

Corresponding author: Ahmet Peker, Department of Radiology, Koç University Hospital, İstanbul, Türkiye

e-mail: doktorpeker@gmail.com

DOI: 10.5152/cjm.2026.25074



Dynamic contrast-enhanced (DCE) MRI has shown greater utility than conventional MRI in differentiating benign from malignant soft tissue tumors. It also contributes significantly to treatment planning, prognosis, therapy monitoring, and follow-up imaging. By offering detailed information on tumor perfusion and vascular permeability, DCE-MRI can enhance biopsy guidance and improve diagnostic accuracy.⁶

This study aimed to evaluate the role of quantitative DCE-MRI parameters and DWI in differentiating the histological grade of STS.

Methods

Study Population

This retrospective study was approved by the Ethics Committee of Koç University (Approval No: 2023.317.IRB1.113, date: October 3, 2023). Given the retrospective nature of the research, the requirement for informed consent was waived by the committee. Between March 2022 and February 2023, patients with histopathologically confirmed STS who underwent preoperative MRI—including DCE-MRI and DWI sequences—were identified from the institutional database.

Inclusion criteria were as follows:

- (1) Histopathologically confirmed diagnosis of STS at the institution;
- (2) Availability of preoperative MRI, including both DCE-MRI and DWI sequences;
- (3) Availability of comprehensive histopathological data, including tumor grade.

Exclusion criteria included:

- (1) History of chemotherapy or radiotherapy before MRI;
- (2) Diagnosis of liposarcoma (due to its unique imaging characteristics and predominant fat content, which may interfere with accurate quantification of imaging parameters);
- (3) Poor image quality due to motion artifacts;
- (4) Predominantly cystic or necrotic tumors.

Imaging Protocol

All imaging was performed using a 3T MRI scanner (Skyra, Siemens Healthcare, Erlangen, Germany). Routine extremity MRI sequences were obtained first, followed by DCE-MRI. For DCE-MRI, 0.1 mmol/kg of gadobutrol (Gadovist) was administered at a rate of 3 mL/s, followed by a 15 mL saline flush. Dynamic contrast-enhanced magnetic resonance imaging was acquired in the axial plane using a spoiled gradient echo T1-weighted sequence with the following parameters: repetition time (TR)/echo time (TE), 5.08/1.77 milliseconds; field of view (FOV), 260 × 192 mm; slice thickness, 3.5 mm; flip angle, 15°; temporal resolution, 7 seconds; and total acquisition time, 255 seconds.

Axial DWI was performed using a single-shot echo-planar imaging sequence with the following parameters: TR/TE, 7000/55 milliseconds; section thickness, 5 mm; b-values of 50, 400, and 800 s/mm²; matrix size, 128 × 128; and fat suppression with spectral adiabatic inversion recovery. Total acquisition time was 3 minutes and 20 seconds.

Image Analysis

Raw data from DWI and DCE-MRI sequences were transferred to a Syngo.via VB60 Multimodality Workplace (Siemens Healthineers, Erlangen, Germany) for post-processing. Dynamic contrast-enhanced magnetic resonance imaging analysis was

performed using a population-based arterial input function (AIF) derived from the Intermediate mode of the built-in model functions, corresponding to the Parker et al population-averaged AIF model. Therefore, no individual artery selection was required. Motion correction was automatically applied by the software and visually verified for each patient. Temporal smoothing was not applied, except when motion-related fluctuations were observed. Baseline T1 values were assumed as 1000 milliseconds, and contrast agent relaxivity (r_1) was set to 4.5 L·mmol⁻¹·s⁻¹. The area under the curve (AUC) was defined as the initial area under the curve within the first 60 seconds (iAUC₆₀) following contrast injection. Perfusion-related parameters (K^{trans} , K_{ep} , V_e , iAUC₆₀) were calculated using the Extended Tofts linear model,¹¹ and color-coded parametric maps were generated. Enhancement curve types were automatically classified into 5 standard curve types (Type 1 – persistent, Type 2 – plateau, Type 3 – washout, Type 4 – flat, and Type 5 – irregular) and visually confirmed by 2 musculoskeletal radiologists.

All examinations were independently reviewed by 2 radiologists (A.P. and Y.E.S.), each with 3 and 4 years of musculoskeletal imaging experience, who were blinded to the histopathological grades. Apparent diffusion coefficient (ADC) values were assessed on ADC maps, and both minimum (ADC_{min}) and average (ADC_{mean}) values were recorded. Dynamic contrast-enhanced magnetic resonance imaging measurements were performed on K^{trans} maps, with regions of interest (ROIs) carefully placed to exclude hemorrhagic, necrotic, and cystic areas. One ROI was positioned over the area with the highest perfusion (K^{trans}_{max}), and a second, broader ROI on the same slice was used to determine average perfusion (K^{trans}_{mean}). This dual approach was chosen to reflect both focal hypervascularity and overall tumor perfusion. Perfusion parameters (K^{trans} , AUC, K_{ep} , V_e) and contrast enhancement curve types were recorded (Figs. 1-3).

For intra-observer reproducibility, measurements were repeated by the same radiologists after a 1-month interval. Both inter- and intra-observer variability analyses were performed, with results summarized in Table 1.

Histological Analysis

All tumors were histopathologically confirmed as STSs and graded according to the French Federation of Cancer Centers Sarcoma Group (FNCLCC) system, which incorporates tumor differentiation, mitotic count, and necrosis. Tumors were classified as grade 1 (low grade), grade 2 (intermediate grade), or grade 3 (high grade). For further analysis, grades 1 and 2 were grouped as “low grade” and compared with grade 3, considered “high grade.”

Statistical Analysis

Statistical analyses were performed using IBM SPSS Statistics version 26 (IBM SPSS Corp.; Armonk, NY, USA). The Shapiro–Wilk test was used to assess the normality of data distribution. Depending on distribution characteristics, comparisons between tumor grades were made using the Mann–Whitney *U*-test, Kruskal–Wallis, and Kolmogorov–Smirnov tests. Fisher’s exact test was used to evaluate associations between categorical variables. To control for multiple comparisons, the Benjamini–Hochberg procedure was applied. Effect sizes (Cohen’s *d*) and 95% CIs were calculated for each significant parameter. Receiver operating characteristic (ROC) analyses were performed for both individual and combined (multiparametric) models to distinguish low- from high-grade sarcomas. The Youden index was used to determine optimal cutoff values, and sensitivity,

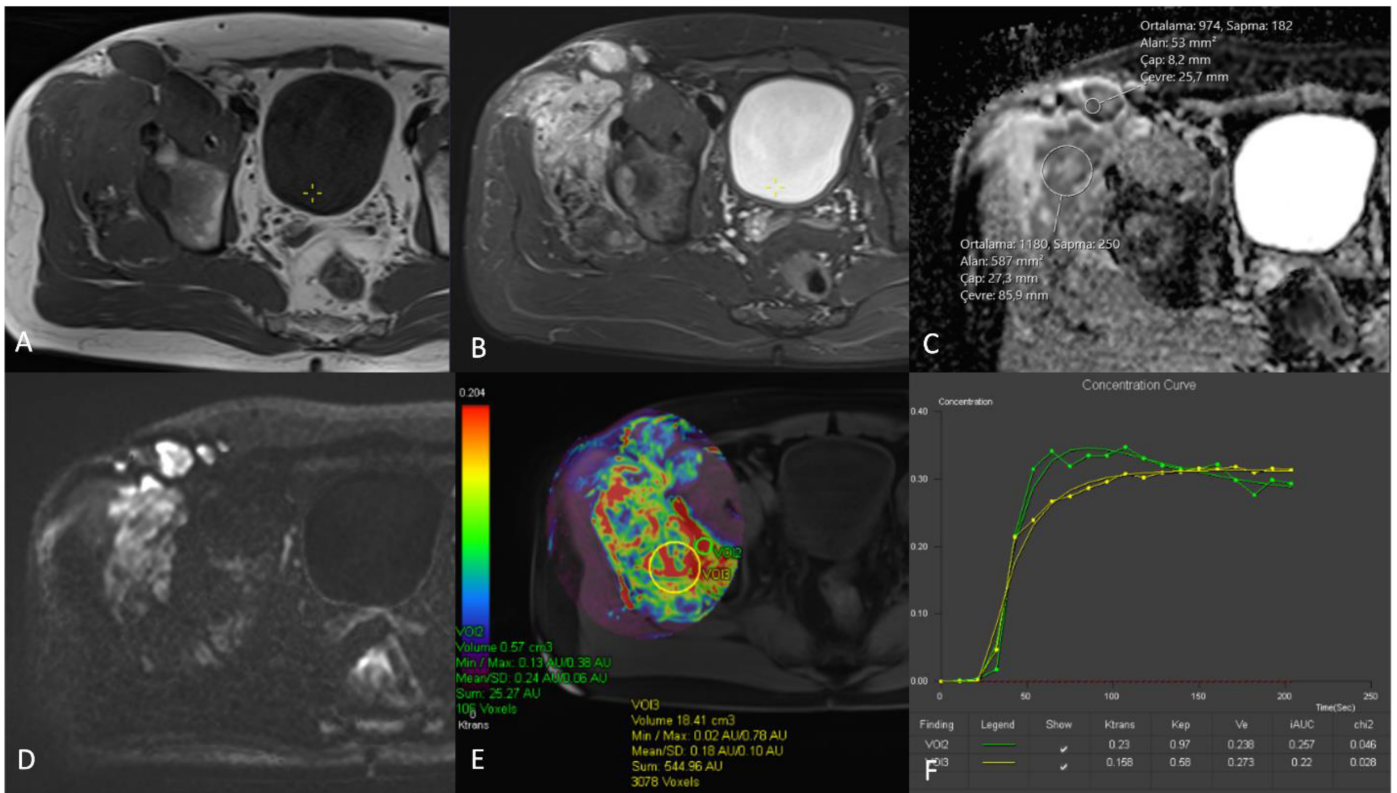


Figure 1. A 42-year-old male patient with myofibroblastic sarcoma (grade 1) of the right proximal thigh. A: axial T1WI. B: axial FS T2WI. C and D: ADC map, DWI (b800). E and F: Ktrans map and dynamic curves.

specificity, positive predictive value (PPV), and negative predictive value (NPV) were calculated. Additionally, a binary logistic regression analysis including tumor size and histologic subtype

as covariates was conducted to identify independent predictors of high-grade disease. A *P*-value <.05 was considered statistically significant after correction.

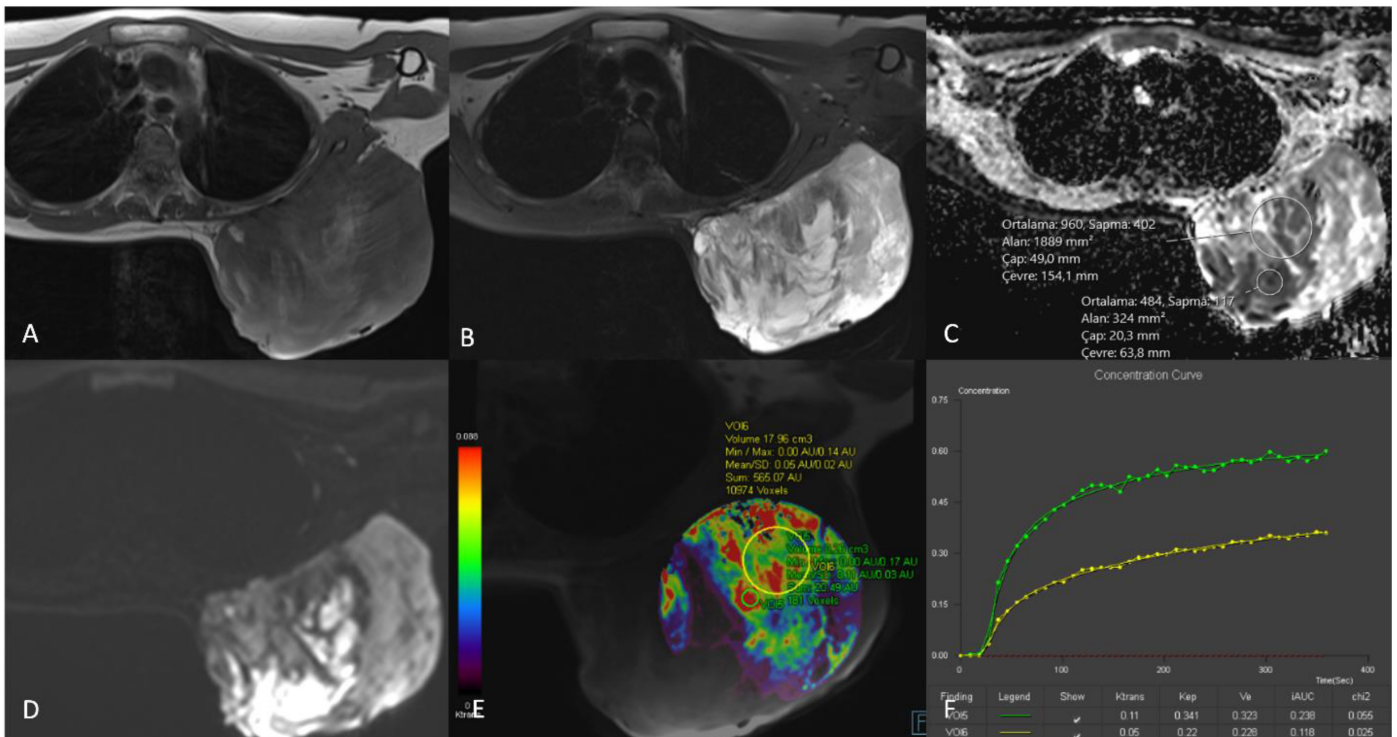


Figure 2. A 23-year-old female patient with synovial sarcoma of the back (grade 3). A: axial T1WI. B: axial FS T2WI. C and D: ADC map, DWI images (b800). E and F: Ktrans map and dynamic curves.

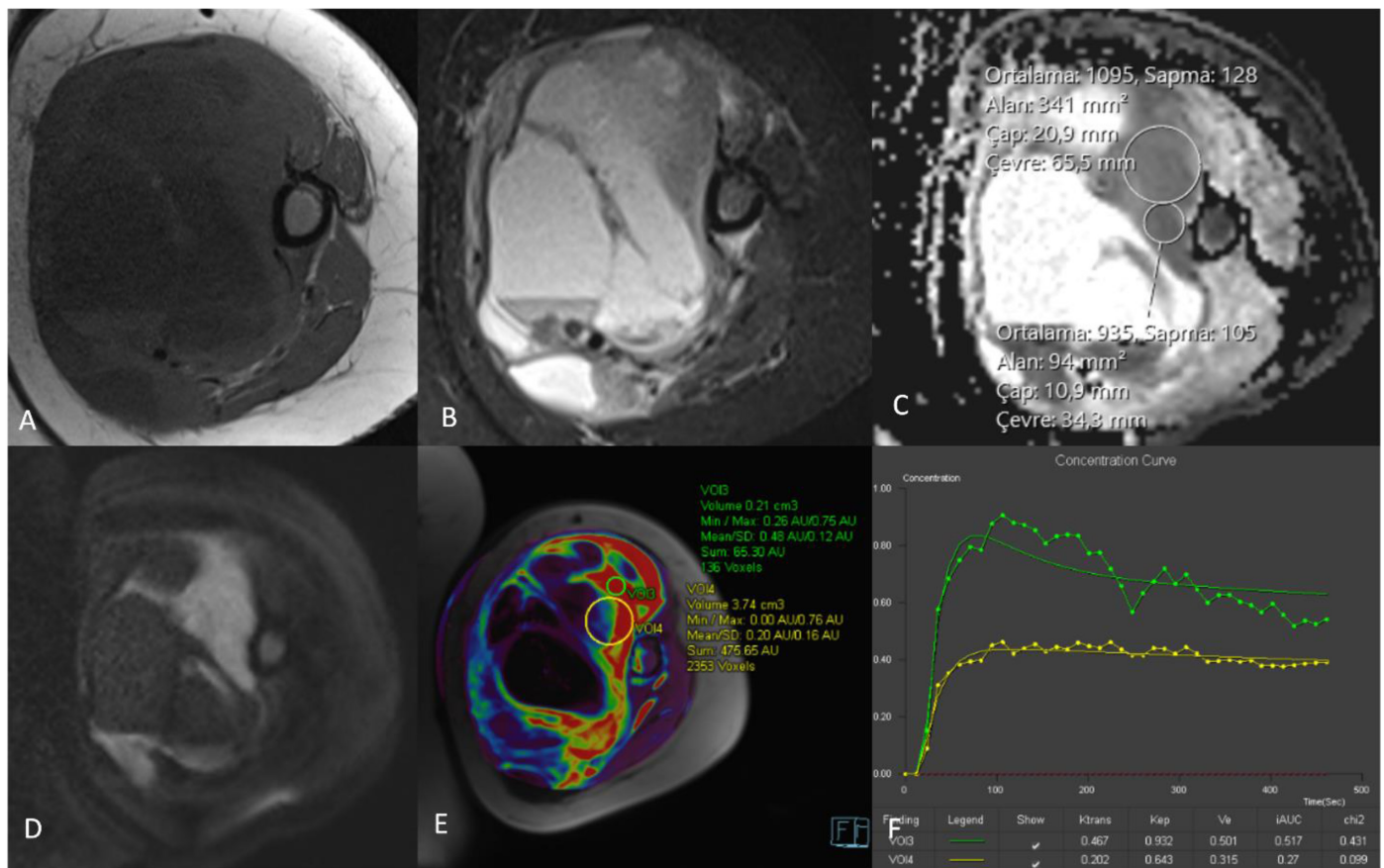


Figure 3. A 56-year-old male patient with undifferentiated pleomorphic sarcoma (grade 3) of the left thigh. A: axial T1WI. B: axial FS T2WI. C and D: ADC map, DWI images (b800). E and F: Ktrans map and dynamic curves.

Results

Patient and Tumor Characteristics

A total of 14 patients (3 females, 11 males) with histopathologically confirmed STSs were included. The mean age was 58.07 ± 16.35 years (range: 23-77 years). According to the FNCLCC grading system, 4 tumors were classified as grade 1, 2 as grade 2, and 8 as grade 3. When regrouped, 6 tumors were categorized as low grade (grades 1 and 2) and 8 as high grade (grade 3).

Histopathological subtypes included undifferentiated pleomorphic sarcoma (n = 5), synovial sarcoma (n = 3), myxofibrosarcoma (n = 2), myofibroblastic sarcoma (n = 1), leiomyosarcoma (n = 1), malignant peripheral nerve sheath tumor (n = 1), and epithelioid sarcoma (n = 1). The mean longest tumor diameter was 113.36 ± 36.87 mm (range: 58-172 mm). The most common tumor locations were the thigh (n = 6), back (n = 3), upper arm (n = 2), calf (n = 2), and shoulder (n = 1). Details regarding histological subtype, pathological grade, anatomical location, tumor size, and patient gender are summarized in Table 2.

No statistically significant differences in age, gender, or tumor size were observed between grade groups (*P* > .05).

Quantitative Dynamic Contrast-Enhanced–Magnetic Resonance Imaging and Diffusion-Weighted Imaging Parameters

When DCE-MRI and DWI parameters were compared across grade 1, 2, and 3 STS, significant differences were found in ADC_{mean} (*P* = .026), ADC_{min} (*P* = .029), and AUC_{max} (*P* = .047); however, after Benjamini–Hochberg correction for multiple

testing, the adjusted *P*-values were .060 for all 3 parameters, indicating a trend toward significance.

When tumors were regrouped into low-grade (grades 1 and 2) and high-grade (grade 3) categories, significant differences were

Table 1. Inter- and Intra-Observer Agreement for Dynamic Contrast-Enhanced Magnetic Resonance Imaging and Apparent Diffusion Coefficient Parameters

Parameter	Intra-Observer ICC (95% CI)	Inter-Observer ICC (95% CI)
Ktrans _{max}	0.91 (0.84-0.96)	0.88 (0.80-0.93)
Kep _{max}	0.89 (0.81-0.95)	0.85 (0.76-0.91)
Ve _{max}	0.87 (0.78-0.93)	0.83 (0.73-0.90)
AUC _{max}	0.90 (0.83-0.95)	0.86 (0.77-0.92)
Ktrans _{mean}	0.87 (0.81-0.91)	0.89 (0.81-0.94)
Kep _{mean}	0.81 (0.74-0.86)	0.77 (0.69-0.83)
Ve _{mean}	0.78 (0.70-0.84)	0.75 (0.66-0.81)
AUC _{mean}	0.82 (0.75-0.86)	0.80 (0.71-0.85)
ADC _{min}	0.94 (0.89-0.97)	0.90 (0.83-0.95)
ADC _{mean}	0.89 (0.84-0.91)	0.79 (0.74-0.86)

ADC, apparent diffusion coefficient; AUC, area under the curve; ICC, intraclass correlation coefficient; Ktrans, volume transfer constant.

Table 2. Demographic and Pathological Characteristics of Included Cases

Diagnosis	Location	Age (Years)	Gender	Pathological Grade	Largest Diameter (mm)
Pleomorphic sarcoma	Cruris	43	M	3	117
Fibromyxosarcoma	Wrist	41	M	1	70
Extraskelletal myxoid chondrosarcoma	Pelvis	82	M	3	76
Low-grade myofibroblastic sarcoma	Pelvis	42	M	1	142
Undifferentiated pleomorphic sarcoma	Arm	60	F	3	167
Soft tissue central chondrosarcoma	Pelvis	67	M	3	120
Undifferentiated synovial sarcoma	Cruris	62	M	3	120
Myofibroblastic sarcoma	Thigh	69	M	1	84
Low-grade spindle cell sarcoma	Thigh	64	F	1	65
Undifferentiated pleomorphic sarcoma	Thigh	56	M	3	120
Synovial sarcoma	Back	23	F	3	180
Myxofibrosarcoma	Pelvis	66	M	2	100
Myxofibrosarcoma	Forearm	56	M	2	150
Myxoid chondrosarcoma	Thigh	82	M	3	76

observed in ADC_{mean} ($P = .027$, Cohen's $d = 0.82$, 95% CI: 0.21-1.41), ADC_{min} ($P = .030$, $d = 0.79$, 95% CI: 0.18-1.37), K^{trans}_{max} ($P = .020$, $d = 0.86$, 95% CI: 0.24-1.47), AUC_{max} ($P = .014$, $d = 0.91$, 95% CI: 0.29-1.50), and K^{trans}_{mean} ($P = .039$, $d = 0.73$, 95% CI: 0.12-1.31). These results are summarized in Table 3.

Receiver operating characteristic analyses demonstrated that ADC_{min} achieved the highest diagnostic accuracy for differentiating low- and high-grade sarcomas (AUC = 0.87, 95% CI 0.75-0.98, $P < .001$), followed by K^{trans}_{max} (AUC = 0.82, 95% CI: 0.69-0.95) and AUC_{max} (AUC = 0.80, 95% CI: 0.66-0.93).

The optimal cutoff values derived from the Youden index were 0.92×10^{-3} mm²/s for ADC_{min} and 0.33 min⁻¹ for K^{trans}_{max},

yielding a sensitivity of 86%, specificity of 81%, PPV of 84%, and NPV of 83% (Table 4).

When multiparametric ROC analysis combining DCE-MRI and DWI parameters was performed, the model yielded an AUC of 0.93 (95% CI: 0.84-0.99, $P < .001$), significantly higher than any single-parameter model (Figure 4).

The calibration plot of this multiparametric logistic regression model demonstrated excellent agreement between predicted and observed probabilities, with the calibration curve closely following the 45° reference line (Hosmer-Lemeshow $P = .42$, Brier score = 0.09) (Figure 4).

In the binary logistic regression analysis, ADC_{min} ($P = .018$) and K^{trans}_{max} ($P = .026$) were identified as independent

Table 3. Comparison of Dynamic Contrast-Enhanced Magnetic Resonance Imaging Perfusion Parameters and Apparent Diffusion Coefficient Values Between Groups

Grade	K ^{trans} _{max} (min ⁻¹)	K ^{ep} _{max} (min ⁻¹)	Ve _{max}	AUC _{max} (a.u.)	K ^{trans} _{mean} (min ⁻¹)	K ^{ep} _{mean} (min ⁻¹)	Ve _{mean}	AUC _{mean} (a.u.)	ADC _{min} ($\times 10^{-3}$ mm ² /s)	ADC _{mean} ($\times 10^{-3}$ mm ² /s)
1 (n = 4)	0.081	0.638	0.238	0.078	0.041	0.363	0.102	0.028	1.52 (±0.71)	1.85 (±0.69)
2 (n = 2)	0.078	0.206	0.414	0.132	0.028	0.134	0.214	0.484	2.04 (±0.52)	2.04 (±0.34)
3 (n = 8)	0.230	0.540	0.323	0.393	0.093	0.481	0.228	0.110	1.24 (±0.38)	0.89 (±0.42)
<i>P</i>	.065	.091	.178	.047	.088	.061	.297	.236	.029	.026
Low/High										
Low (n = 6)	0.049	0.520	0.199	0.111	0.32	0.278	0.126	0.056	1.70 (±0.65)	2.05 (±0.26)
High (n = 8)	0.230	0.540	0.244	0.393	0.91	0.481	0.228	0.118	0.89 (±0.38)	1.24 (±0.42)
<i>P</i>	.020	.302	.245	.014	.039	.070	.245	.196	.03	.027

ADC, apparent diffusion coefficient; AUC, area under the curve; K^{trans}, volume transfer constant. Bold values indicate statistically significant differences between groups ($p < 0.05$).

Table 4. Diagnostic Performance of Quantitative Dynamic Contrast-Enhanced Magnetic Resonance Imaging and Diffusion-Weighted Imaging Parameters for Distinguishing High-Grade from Low-Grade Soft Tissue Sarcomas. Diagnostic performance metrics derived from ROC analysis and Youden index–based optimal cutoffs

Parameter	Cutoff	Sensitivity (%)	Specificity (%)	PPV (%)	NPV (%)	Accuracy (%)
ADC_min ($\times 10^{-3}$ mm ² /s)	0.92	86	81	84	83	85
Ktrans_max (min ⁻¹)	0.33	84	78	82	80	82
AUC_max (a.u.)	1.45	80	76	78	78	78
Multiparametric model	–	89	86	88	87	88

The multiparametric model combines ADC_min, Ktrans_max, and AUC_max values to improve diagnostic accuracy.

ADC, apparent diffusion coefficient; AUC, area under the curve; Ktrans, volume transfer constant; NPV, negative predictive value; PPV, positive predictive value.

predictors of high-grade sarcoma, after adjustment for tumor size and histologic subtype.

When maximum perfusion enhancement curve types were evaluated, the following distribution was noted:

- Grade 1 STS: Type 2 in 2 cases (50%), Type 3 in 1 case (25%), and Type 4 in 1 case (25%).
- Grade 2 STS: Type 2 in all cases (100%).
- Grade 3 STS: Type 3 in 4 cases (50%), Type 4 in 3 cases (37.5%), and Type 5 in 1 case (12.5%).

No statistically significant difference in enhancement curve types was found between histopathological grade groups.

Discussion

Our findings revealed significant differences in key DCE-MRI perfusion parameters (Ktrans_max, AUC_max, and Ktrans_mean) and ADC values (ADC_min and ADC_mean) between low-grade and high-grade STS. High-grade tumors demonstrated significantly higher perfusion values and lower ADC values, reflecting their more aggressive biological behavior.

The elevated perfusion parameters observed in high-grade STS likely reflect increased vascularity and angiogenesis. Ktrans, representing the volume transfer constant between plasma and the extravascular extracellular space, quantitatively indicates vascular permeability and perfusion.¹² Elevated Ktrans values in high-grade tumors suggest more active angiogenesis, a hallmark of tumor aggressiveness.^{3,13}

This study adds to the growing body of evidence on the role of multiparametric MRI in STS grading. Previous studies have demonstrated the value of DCE-MRI and DWI in differentiating benign from malignant soft tissue lesions and in estimating tumor grade.^{6,8,11,14} These results further support these findings, showing that quantitative perfusion metrics—particularly Ktrans_max and AUC_max—provide complementary diagnostic information to DWI-derived ADC parameters.

The lower ADC values observed in high-grade tumors are consistent with prior research linking restricted diffusion to increased tumor cellularity, reduced extracellular space, and higher nuclear-to-cytoplasmic ratios.^{2,4,7,9} Nagata et al⁸ reported that ADC values were significantly lower in high-grade STS than in low-grade, identifying a cutoff of 1.1×10^{-3} mm²/s with 82.9% sensitivity and 80.0% specificity. These findings on ADC_min closely mirror these results.

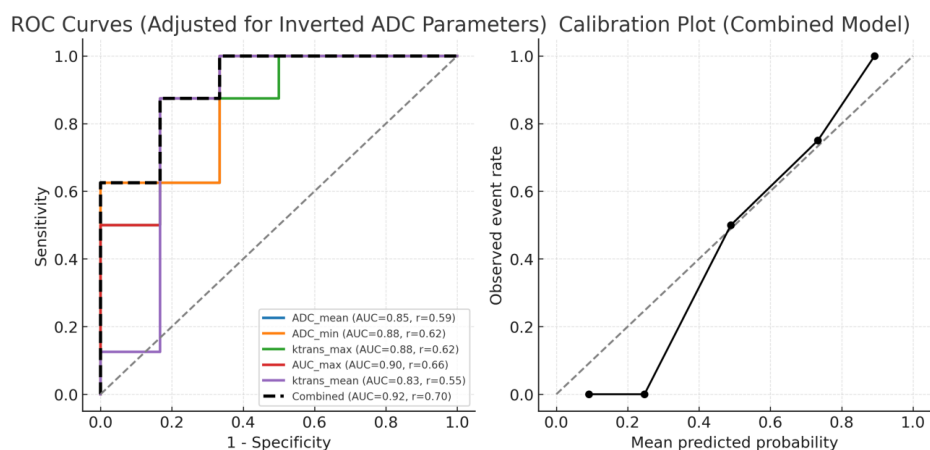


Figure 4. Receiver operating characteristic (ROC) curves and calibration plot for quantitative DCE-MRI and DWI parameters in differentiating low- and high-grade soft tissue sarcomas. ROC curves demonstrate the diagnostic performance of individual parameters (ADC_mean, ADC_min, Ktrans_max, AUC_max, and Ktrans_mean) and the combined multiparametric logistic regression model. For ADC parameters, values were inverted ($-ADC$) to reflect the inverse relationship between ADC and tumor grade, where lower ADC values indicate higher grade. The left panel shows single-parameter and combined ROC curves with corresponding AUC and effect size (r) values. The right panel presents the calibration plot for the combined model, illustrating good agreement between predicted and observed probabilities. In the calibration plot, predicted probabilities closely matched the observed event rates, indicating good model calibration (Hosmer–Lemeshow $P > .05$).

Importantly, this analysis showed that ADC_{min} outperformed ADC_{mean} in distinguishing between low- and high-grade STS. This supports the findings of Zou et al,¹⁴ who suggested that ADC_{min} may better reflect the most aggressive components within heterogeneous tumors. Since ADC_{min} is more sensitive to regions of highest cellularity, it may serve as a more accurate marker of tumor grade than ADC_{mean}.

Recent multiparametric approaches—including ultrafast DCE-MRI, ADC histogram analysis, and radiomics-based models—have also shown promise for non-invasive grading and prognostication in STS.^{15,16} For instance, a recent systematic review reported that MRI-based radiomics achieved a pooled AUC of approximately 0.91 for STS grading.¹⁶ Although these advanced techniques were beyond the scope of the present study, these results are in line with this trend and further highlight the potential of quantitative MRI biomarkers for tumor characterization and individualized treatment planning.

Beyond its potential role in tumor grading, DCE-MRI also has substantial clinical utility in the postoperative follow-up of patients with STSs. In daily practice, quantitative perfusion analysis helps differentiate residual or recurrent tumor from postoperative granulation or scar tissue, which often present with overlapping findings on conventional MRI. By demonstrating increased vascularity and perfusion in viable tumor tissue, DCE-MRI can reduce false-positive interpretations and potentially decrease unnecessary biopsies.¹⁷

Several limitations must be acknowledged. First, the retrospective design and small sample size—particularly the limited number of grade-2 cases—restrict generalizability. Second, the histological heterogeneity of included STS subtypes may have introduced variability in imaging features. Third, partial volume effects and ROI selection bias may have affected the quantitative measurements. Additionally, whole-lesion histogram or radiomics analysis was not performed, which could have provided a more comprehensive assessment of intratumoral heterogeneity. Fourth, liposarcomas were excluded due to their distinct imaging characteristics, which limit applicability to this common STS subtype. Fifth, the single-center design and lack of external validation limit reproducibility across different imaging platforms and institutions. Lastly, despite statistically significant group differences, overlap in parameter values may reduce diagnostic accuracy in individual cases. Future prospective multicenter studies with standardized DCE-MRI settings (temporal resolution, AIF definition) and whole-lesion radiomics approaches are warranted to improve clinical applicability and generalizability.

Despite these limitations, this study provides valuable preliminary insights into the utility of quantitative DCE-MRI and DWI in preoperative STS grading. Future prospective studies with larger cohorts and standardized imaging protocols are essential to validate these results and establish reliable cutoff values for clinical use.

This study demonstrates that quantitative DCE-MRI parameters (K_{trans}_{max}, AUC_{max}, and K_{trans}_{mean}) and ADC values (ADC_{min} and ADC_{mean}) differ significantly between low-grade and high-grade STS. These metrics may serve as useful non-invasive imaging biomarkers for preoperative tumor grading, potentially complementing or even reducing reliance on biopsy. The integration of multiple quantitative MRI parameters could enhance the accuracy of non-invasive tumor assessment. However, validation through larger, prospective studies is required to support clinical implementation.

Data Availability Statement: The data that support the findings of this study are available on request from the corresponding author.

Ethics Committee Approval: Ethical committee approval was received from the Ethics Committee of Koç University (Approval No.: 2023.317.IRB1.113; Date: 03.10.2023).

Informed Consent: The requirement for informed consent was waived by the Ethics Committee because of the retrospective nature of the study.

Peer-review: Externally peer-reviewed.

Author Contributions: Concept – A.P., Y.E.S., H.O.A.; Design – A.P., A.H.C., E.M.C., Y.E.S.; Supervision – Y.E.S.; Materials – A.H.C., E.M.C., H.O.A.; Data Collection and/or Processing – A.P., Y.E.S., H.O.A., A.H.C., E.M.C.; Analysis and/or Interpretation – A.P., Y.E.S., E.M.C.; Literature Review – A.P., A.H.C.; Writing – A.P., A.H.C., H.O.A.; Critical Review – Y.E.S., H.O.A., E.M.C.

Declaration of Interests: The authors have no conflict of interest to declare.

Funding: The authors declared that this study has received no financial support.

References

- Crombé A, Kind M, Fadli D, et al. Soft-tissue sarcoma in adults: imaging appearances, pitfalls and diagnostic algorithms. *Diagn Interv Imaging*. 2023;104(5):207-220. [\[CrossRef\]](#)
- Chhabra A, Ashikyan O, Slepicka C, et al. Conventional MR and diffusion-weighted imaging of musculoskeletal soft tissue malignancy: correlation with histologic grading. *Eur Radiol*. 2019;29(8):4485-4494. [\[CrossRef\]](#)
- Van Den Berghe T, Verstraete KL, Lecouvet FE, Lejoly M, Dutoit J. Review of diffusion-weighted imaging and dynamic contrast-enhanced MRI for multiple myeloma and its precursors (monoclonal gammopathy of undetermined significance and smoldering myeloma). *Skelet Radiol*. 2022;51(1):101-122. [\[CrossRef\]](#)
- Filograna L, Magarelli N, Cellini F, et al. Diffusion weighted imaging (DWI) and apparent diffusion coefficient (ADC) values for detection of malignant vertebral bone marrow lesions. *Eur Rev Med Pharmacol Sci*. 2018;22(3):590-597. [\[CrossRef\]](#)
- Gowda P, Bajaj G, Silva FD, Ashikyan O, Xi Y, Chhabra A. Does the apparent diffusion coefficient from diffusion-weighted MRI imaging aid in the characterization of malignant soft tissue tumors and sarcomas. *Skelet Radiol*. 2023;52(8):1475-1484. [\[CrossRef\]](#)
- Li X, Wang Q, Dou Y, et al. Soft tissue sarcoma: can dynamic contrast-enhanced (DCE) MRI be used to predict the histological grade? *Skelet Radiol*. 2020;49(11):1829-1838. [\[CrossRef\]](#)
- Lin X, Lee M, Buck O, et al. Diagnostic accuracy of T1-weighted dynamic contrast-enhanced-MRI and DWI-ADC for differentiation of glioblastoma and primary CNS lymphoma. *AJNR, Am J Neuroradiol*. 2017;38(3):485-491. [\[CrossRef\]](#)
- Nagata S, Nishimura H, Uchida M, et al. Diffusion-weighted imaging of soft tissue tumors: usefulness of the apparent diffusion coefficient for differential diagnosis. *Radiat Med*. 2008;26(5):287-295. [\[CrossRef\]](#)
- Park GE, Jee WH, Lee SY, et al. Differentiation of multiple myeloma and metastases: use of axial diffusion-weighted MR imaging in addition to standard MR imaging at 3T. *PLOS One*. 2018;13(12):e0208860. [\[CrossRef\]](#)
- Singer AD, Pattany PM, Fayad LM, Tresley J, Subhawong TK. Volumetric segmentation of ADC maps and utility of standard deviation as measure of tumor heterogeneity in soft tissue tumors. *Clin Imaging*. 2016;40(3):386-391. [\[CrossRef\]](#)
- Seo M, Choi Y, Soo Lee Y, et al. Glioma grading using multiparametric MRI: head-to-head comparison among dynamic susceptibility contrast, dynamic contrast-enhancement, diffusion-weighted images, and MR spectroscopy. *Eur J Radiol*. 2023;165:110888. [\[CrossRef\]](#)
- Sourbron SP, Buckley DL. Classic models for dynamic contrast-enhanced MRI. *NMR Biomed*. 2013;26(8):1004-1027. [\[CrossRef\]](#)
- Tofts PS, Kermode AG. Measurement of the blood-brain barrier permeability and leakage space using dynamic MR imaging. 1. Fundamental concepts. *Magn Reson Med*. 1991;17(2):357-367. [\[CrossRef\]](#)
- Zou Y, Wang QD, Zong M, Zou YF, Shi HB. Apparent diffusion coefficient measurements with diffusion-weighted imaging for differential diagnosis of soft-tissue tumor. *J Cancer Res Ther*. 2016;12(2):864-870. [\[CrossRef\]](#)

15. Guo Y, Zhu Y, Xu Y, et al. Radiomics and machine learning for the prediction of soft-tissue sarcoma histologic grade using MRI. *Eur Radiol.* 2021;31(7):4361-4372. [\[CrossRef\]](#)
16. Cao L, Liu Z, Li M, Chen H, et al. MRI-based radiomics in grading soft-tissue sarcomas: a systematic review and meta-analysis. *Eur J Radiol.* 2024;176:111237. [\[CrossRef\]](#)
17. Oka K, Yakushiji T, Sato J, Hirai T, Yamashita Y. Dynamic contrast-enhanced MRI for differentiating postoperative recurrent soft-tissue sarcoma from benign granulation tissue: quantitative analysis improves diagnostic confidence. *Eur Radiol.* 2019;29(1):273-283. [\[CrossRef\]](#)